International Journal of Systems Signal Control and Engineering Application
MEDWELL PUBLICATIONS

MPPT Controller Simulation for a Boost DC/DC Converter used in Fuel Cell Electric Vehicle

[1]Arvin Ghasemi and [2]Seyed Mohammad Taghi Nabavi Razavi
[1]*Department of Power Engineering, Electrical Engineering, Islamic Azad University of Qazvin, Qazvin, Iran*
[2]*Islamic Azad University of Qazvin, Qazvin, Iran*

Key words: Hybrid vehicle, fuel cell, electric vehicle, Maximum power point tracking

Corresponding Author:
Arvin Ghasemi
Department of Power Engineering, Electrical Engineering, Islamic Azad University of Qazvin, Qazvin, Iran

Page No.: 153-164
Volume: 10, Issue 6, 2017
ISSN: 1997-5422
International Journal of Systems Signal Control and Engineering Application

Abstract: Recently, the fuel cell electric vehicles have attracted many research interests. This study examines the performance of MPPT-FC generators to provide power in electronic devices by increasing the voltage level of the boost DC/DC converter. In this model, the maximum power in Fuel Cell generators (FC) based on integrated control algorithms of boost DC/DC converter are used. In MPPT method, the rapid changes raise in power output of fuel cells but it shortens the life of fuel cells and the destruction of these cells and reduction in system performance. To fix the problem, air production control system has been designed to improve quality of output power and avoid the phenomenon of lack of receiving energy during rapid power transitions. This has been obtained by modeling and simulating power of the fuel cells from the vehicles with experimental data in the same models. Use of power of fuel cells has been targeted in reducing cost and reducing consumption of micro controllers in use of boost DC/DC converter in MPPT-FC models. These micro controllers aim at using the measurements from power of fuel cells to determine ratio coefficient of control signals in boost DC/DC converter. Then, a DC-DC boost converter positioned to divide the current in high power application in fuel cell is recommended and then MPPT controller is designed and simulated for a boost DC/DC converter used in electrical devices of fuel cell and the simulated circuit with and without presence of MPPT has been compared and results from simulation for various loads have been examined. Ultimately, the obtained results are analyzed.

INTRODUCTION

In today's world, energy and fuel consumption refers to an important topic of hot debate. For years consumption of alternative fuels instead of fossil fuels in a variety of energy devices has been examined. This is also true for vehicle as a major consumer of fuel and energy. In recent years, vehicles have been made which use alternative energy such as solar energy, CNG and natural gas, electrical energy, hydrogen, LPG instead of

gasoline. Further, the vehicles have been produced that use combined both types of these energies, called hybrid vehicle. Hybrid technology is superior due to making it easier than fuel cell, greater range and less weight than electric motor and lower fuel consumption and emissions than combustion engine (Dwari and Parsa, 2007). In general, a vehicle which has two or several source to generate power is called hybrid vehicle. Yet, since, a type of hybrid in which an internal combustion engine has been combined with Gasoline or diesel fuel with an electrical engine, they are used in today's vehicles; usually, whenever it is talked on a hybrid vehicle, it means this type of vehicle, called with hybrid electric vehicle (Samosir and Yatim, 2008). The transport industry in particular is dependent on the use of fossil fuels. By reducing sources of fuel, the use of alternative fuels became important. Fuel cells are included of power sources with high-density and utilize a renewable fuel such as hydrogen for primary energy. Thus, Fuel cells are often recognized as a convenient alternative for public applications such as personal vehicles due to emissions reduction (Samosir and Yatim, 2010, 2011). A variety of fuel cells have caused creation of a variety of methods in various classifications. Indeed, it can classify fuel cells based on the combined action of electrolytic cells. The proton exchange of membrane (layers) of fuel cells has raised large properties for applications of vehicles due to the following reasons:

- Performance at a lower temperature which causes them to turn off faster
- Less pressure that it raises the safety factor
- It can easily adjust function of system
- Lower emissions and higher conversion efficiency

Fuel cell electric vehicles will be known as an alternative to conventional vehicles in the near future. In this research, the proton exchange of fuel cells membrane as the basic energy system and a supercapacitor and/or battery to store a rechargeable energy is used.

Basic energy system has increased driving range and chargeable energy storage is used in the acceleration and brake systems of car. DC-DC converters can be used as interface in the part of electrical power to increase the voltage level between the equipment. Due to the limitations of the vehicle, the converter structure must be reliable in terms of vehicle performance, low size and weight with high efficiency, low electro-magnetic interference, low current and voltage ripple. In addition, electric vehicles cells face many challenges such as lower cost, lower fuel consumption, less waste of catalysts, less analysis of carbon existing in ripples and longer life. Boost DC/DC converter is used to resolve these limitations simultaneously at vehicle. For this, these converters are largely used regarding their capabilities in performance of fuel cells in current control function mode and permanent function mode and increase in efficiency of these cells (Samosir and Yatim, 2011; Thounthong *et al*., 2009). High ripple currents in fuel cells have caused abundant disadvantages including increased fuel consumption, loss of momentum and the loss of support carbons in electric cells and disruption and imbalances under overload. Boost DC/DC converter model is a suitable candidate to face these challenges. Indeed, in this model, high power and increased reliability at system come to realize (Van Der Broeck and Tezcan, 2006). Boost DC/DC converter model regarding its capabilities is recognized as a suitable solution with the benefits included of high efficiency, less voltage ripple and smaller filter components.

MATERIALS AND METHODS

Analysis of boost DC/DC converter model: In this analysis, we have assumed neglecting cells resistance and increased capacitor filter to a sufficient extent in order that the ripple voltage passes through it to a lesser extent compared to DC voltage. In this analysis, it has been assumed that all the semiconductor elements have been considered to an ideal state, e.g., they have zero impedance at turned on mode and infinite impedance in turned off mode. Output current waveform analysis in permanent operation for three cases has been attributed as a function of the value. Input ripple current at boost DC/DC converter is expressed as follow:

$$\Delta i_{fc} = \begin{cases} \frac{V_{bus}}{L}(1-3\alpha)\alpha T \times 0 \le \alpha \le T/3 \\ \frac{V_{bus}}{L}(2-3\alpha)\left(\alpha - \frac{1}{2}\right)T \times T/3 \le \alpha \le 2T/3 \\ \frac{V_{bus}}{L}(3-3\alpha)\left(\alpha - \frac{2}{3}\right)T \times 2T/3 \le \alpha \le T \end{cases} \quad (1)$$

Maximum ripple current is as follow:

$$\Delta i_{fc}\Big|_{\alpha=\frac{1}{2}\times\alpha=\frac{1}{2}\times\alpha=\frac{5}{6}} = \frac{V_{bus}}{12LF} \quad (2)$$

It can obtain inductance L regarding equation:

$$L \ge \frac{V_{busmax}}{12\Delta i_{fcmax} f} \quad (3)$$

where, DC bus voltage has maximum voltage value:

$$V_{bus} = V_{busmax} \quad (4)$$

Ripple current Δi_{fcmax} has been designed as a measurement criterion and it should pay attention to this point that the designed inductance is 25% of inductance with plug of DC-DC converter boost for the same Δi_{fcmax} ripple current and the same switching frequency, i.e., the inductance value is 25% of the inductance of the used converter.

Modeling fuel cells: The proton exchange of fuel cells is a new technology for a variety of vehicle applications due to high efficiency and production of low greenhouse gases and direct electricity generation without any interface (Ellabban *et al*., 2011). The proton exchange of fuel cells refers to a converter system which converts the chemical energy used in fuel cells to electrical energy. The input is the load current in the proton model and the output is the voltage produced by means of proton exchange model of fuel cells. The output voltage of these cells is defined as follow (Benyahia *et al*., 2014):

$$V_{fc} = n_{fc} V_{cll} = n_{fc}\left(E_{nernst} - E_{Act} - E_{con} - E_{ohm}\right) \quad (5)$$

where, E_{nernst} (Nernst voltage) represents Thermodynamic potential of Recursive storage voltage of fuel cells, calculated via. Nernst equation at standard degree represented in reference (Kim *et al*., 2011). E_{acr} represents active voltage drop which the voltage drop is during driving with vehicle; the voltage drop is generated during vehicle driving. The general form of this voltage drop is defined via. Tafel equation. E_{con} represents the voltage related to concentration of lead acid in fuel cells which is defined regarding Faraday's law (Seyezhai and Mathur, 2012). E_{ohm} represents Ohmic voltage drop which raises the value of voltage to resistance against the current of electrons in the electrodes of fuel cells and resistance against the current made of ions at fuel cells layers. It indicates the resistance between fuel membranes and electrodes during the current movement (Torreglosa *et al*., 2011). Equation 5 can be calculated via. the equations:

$$E_{nernst} = 1.229\text{-}8.5e^{-5}\left(T_{fc}\text{-}298.15\right) + 4.308e^{-5}\left[In\left(P_{H2}\right) + \frac{1}{2}In\left(P_{O2}\right)\right] \quad (6)$$

$$E_{act} = \frac{RT}{\propto ZF} In\left(i_{fc}/I_{O}\right) = T_{fc}\left[a + bIn\left(i_{fc}\right)\right] \quad (7)$$

$$E_{con} = -0.016\ In\left(1 - \frac{i_{fc}}{25}\right) \quad (8)$$

$$E_{ohm} = i_{fc} R_{ohm} \quad (9)$$

where, R_{ohm} represents internal electrical resistance and defined as a function of electrical conductivity and the temperature of electric cell:

$$R_{ohm} = \frac{t_m}{\sigma_m} \quad (10)$$

where, σ_m, t_m represent membrane thickness and electrical conductivity, the electrical conductivity is defined as follow:

$$\sigma_m = \left(0.005139\lambda_m\text{-}0.00326\right)e^{\left(1.155\cdot\frac{350}{T_{fc}}\right)} \quad (11)$$

where, λ_m depends on membrane water content, considered as the parameter in this article; value of λ_m ranges from 0-14 and equivalents to moisture between 0-100%. Under maximum supersaturation, value of λ_m might reach to the highest value (Eq. 23). In addition, λ_m can be under influence of the process of preparing the relevant membrane such membrane preparation through injecting hydrogen and oxygen gases and the time to use membrane. The dynamic model of the gas transmission can describe various pressure modes during fuel cell operation. The associated equations can describe the value of input and output hydrogen and oxygen value in fuel cells.

$$\frac{dpca}{dt} = \frac{RT_{fc}}{V_{ca}}\left(W_{ca,\,in}\text{-}W_{ca,\,out}\text{-}W_{ca,\,rec}\right) \quad (12)$$

where, $W_{ca,\,rec}$, $W_{ca,\,in}$, $W_{ca,\,out}$ represent Oxygen consumption rates, Cathode mass flow and cathode output mass flow:

$$W_{ca,rec} = M_{O2}\frac{n_{fc} i_{fc}}{4F} \quad (13)$$

$$W_{ca,\,in} = \frac{1}{1+w_{atm}} W_{in} \quad (14)$$

$$W_{atm} = \frac{M_v}{M_a} \times \frac{\varnothing_{atm} P_{sat}\left(T_{atm}\right)}{P_{atm}\text{-}\varnothing_{atm} P_{sat}\left(T_{atm}\right)} \quad (15)$$

$$W_{in} = K_{ca,\,in}\left(P_{sm}\text{-}P_{ca}\right) \quad (16)$$

$$W_{ca,rec} = K_{ca,\,out}\left(P_{ca}\text{-}P_{rm}\right) \quad (17)$$

where, M_a, M_w, φ_{atm} represent molar mass of steam and air and relative humidity under environmental conditions and $K_{ca,\,out}$, $K_{ca,\,in}$, W_{atm} represent ratio of moisture at the fixed input opening of cathodes and fixed output opening of cathodes as follow. The angular velocity W_{cp} is defined by the differential equation:

$$\frac{dW_{cp}}{dt} = \frac{1}{J_{cp}}\left(\tau_{cm} - \tau_{cp}\right) \quad (18)$$

J_{cp} represent inertia of the motor and compressor and τ_{op}, τ_{om} represent the compressor motor torque and load torque required to conduct the compressor:

$$\tau_{cm} = \frac{K_t \eta_{cm}}{R_{cm}}\left(V_{cm} - K_v W_{cp}\right) \quad (19)$$

$$\tau_{cp} = \frac{C_p T_{atm}}{\eta_{cp} w_{cp}}\left[\left(\frac{p_{sm}}{p_{atm}}\right)^{\frac{r}{r-1}} - 1\right] W_{cp} \quad (20)$$

where, R_{cm} and K_V, K_t represent the motor constants, η_{cp} represents return and efficiency of compressor, η_{cm} represents mechanical efficiency of motor, C_p represents specific heat capacity of air, V_{cm} represents voltage of compressor motor and Wcp represents compressor mass flow. The air pressure at several converter plugs is as follow:

$$\frac{dpsm}{dt} = \frac{RT_{cp}}{M_a V_{sm}}\left(W_{cp} - W_{in}\right) \quad (21)$$

Total net power of fuel cells (P_{net}) is calculated as follows:

$$P_{net} = P_{fc} \times P_{cm} \quad (22)$$

$$P_{fc} = V_{fc} \times i_{fc} \quad (23)$$

$$P_{cm} = \frac{k_t}{R_{cm}}\left(V_{cm} - K_v W_{cp}\right) \quad (24)$$

where, P_{fc} represents power of fuel cell which generates fuel cell Voltage V_{fc} and fuel cell current i_{fc} and P_{cm} represents the power related to compressor. One of the problems in the proton exchange system of fuel cell membrane is the amount of power produced via. this system. The extent of increase in power of fuel cells caused increase in T_{fc} and content of water membrane λ_m. A control strategy of a MPPT which has a fast response of its characteristics can produce the electrical power at any membrane content properly. To resolve these problems, MPPT converter is required. The used MPPT algorithm has been made simply via. experimental method. In this algorithm, cycle is gained via change in constant values and efficiency of system. In addition, proton exchange system avoids membranes arisen in system via. the air consumption control. The studies on this issue which relates to the oxygen pressure level in cathodes have been conducted by Tang *et al*. (2011) successfully via. a control method which is the compressor motor voltage in which a control system on compressor has been used which uses the current measurement at solar cells. A dynamic or fixed function affiliated to the input values at stable mode V_{fc} and fuel cell current i_{cm} can be used in this method. However this method suffers from numerous sensivities to the environmental conditions, Propotational Integrator (PI) is used to increase reliability and resolve this sensitivity used in control of control of oxygen pressure ratio and function feedback.

Modeling Supercapacitors: Due to needing regenerative powers in the devices which work with fuel cells, a variety of super capacitors that are in connection with renewable power sources are used. This includes energy storage devices such as batteries and super capacitors. Super capacitors are a practical solution to improve the performance of proton exchange devices of fuel cells to increase the reliability of the rapid response at transient mode in vehicles which have higher power and longer lifetime compared to battery. These studies aim to model super capacitors mentioned in abundant studies which can be divided into two groups: the first group of these devices is the nonlinear circuit capacitors mentioned in Rekioua *et al*. (2014), Benyahia *et al*. (2013), yet, the second group of capacitor model is expressed linearly or the model without change during the modeling process of its various parts (Rekioua and Matagne, 2012). This model has been recognized with its preciseness however more time is required to implement it at software due to its fixed and linear parameters. The super capacitor model presented in this study is based on simple model (RC) to store energy at capacitor (Benyahia *et al*., 2013; Rekioua and Matagne, 2012). This model includes a nonlinear capacitor E_{sr} and C_{Vso} and basic Capacitor C_0. The parameters of model have been expressed using certain constants of the test and experimental method by Benyahia *et al*. (2014).

RESULTS AND DISCUSSION

Analysis of the simulated circuit and study on it for various loads: The simulated circuit includes two parts, i.e., the first part of the circuit is the main simulation and the second part is the control circuit in which there is the Maximum power point tracking in this study, we analyze the main circuit with MPPT control circuit as well as without MPPT control circuit and examine the response of circuits and then analyze MPPT circuit and examine it for various R, RL, RC, RLC loads. In this simulation, values of all cells equal to L= 9 mh and capacitors equal to C = 180 f and load equals to R = 10 Ω. The simulated main circuit in MATLAB has been represented in Fig. 1:

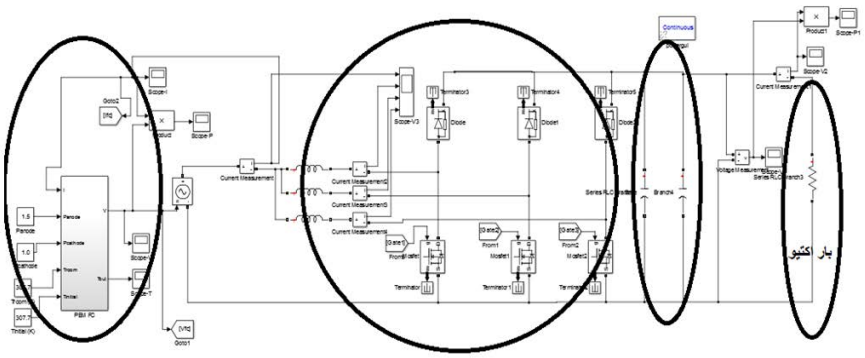

Fig. 1: The simulated main model

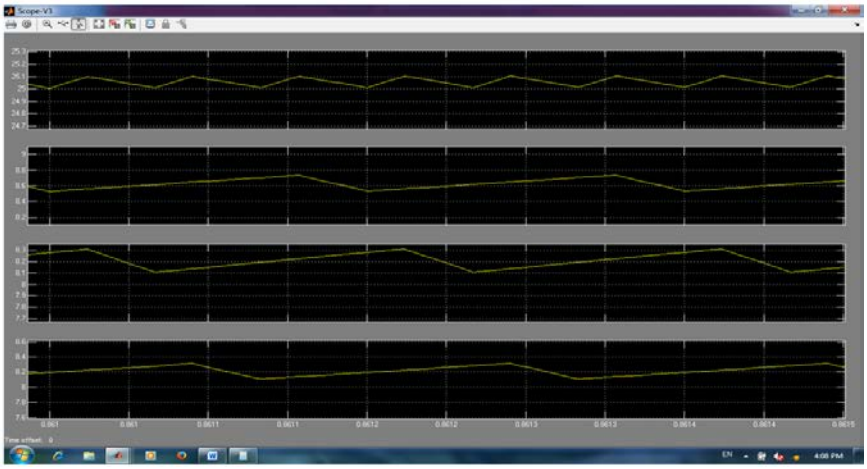

Fig. 2: The current passing cells L_1, L_2, L_3 as well as sum of them to time

- Fuel cell is at the first left side which consists of the input variables of fuel cell
- I: fuel cell current
- Panode: gas pressure at anode to atmosphere direction
- Pcathode: gas pressure at cathode to atmosphere direction
- Troom: room temperature and/or the environment in which cell exists in terms of Kelvin
- Tinitial: the initial temperature of fuel cell which has been assumed with the same environment temperature at this simulation

Output variables of fuel cell: V: output terminal voltage, Tout: temperature of fuel cell during operation. In following, after placing the alternating voltage source and current measurement, the cells are placed which have task to take the input current fluctuations and then the current measurement has been reused and the currents at fuel cell have been examined (Fig. 2). There is the inverter converter at the next section which has consisted of three diodes and three MOSFETs with the task to increase voltage from 12-13 V-55 V in the circuit, i.e., it has made the task of Trans at circuit ac (Fig. 3).

In following, there are two parallel capacitors which are to take the output voltage fluctuations and the resistive load has been placed at the end; the output current and load-side power are observed below the output voltage (Fig. 4 and 5).

It should be noted that the first peak is observed that the load side power, voltage and load side current scopes and this is for two reasons that the first is all the values are considered equal to 0 at the beginning of simulation and the second reason is the programming error and numerical solution to guess the best response or the initial guess for Maximum power point tracking to gain the stationary mode.

Control circuit and MPPT circuit: Output voltage and output current of fuel cell are entered into MPPT and output voltage and output current of fuel cell are entered into MPPT and then transmitted after multiplying by

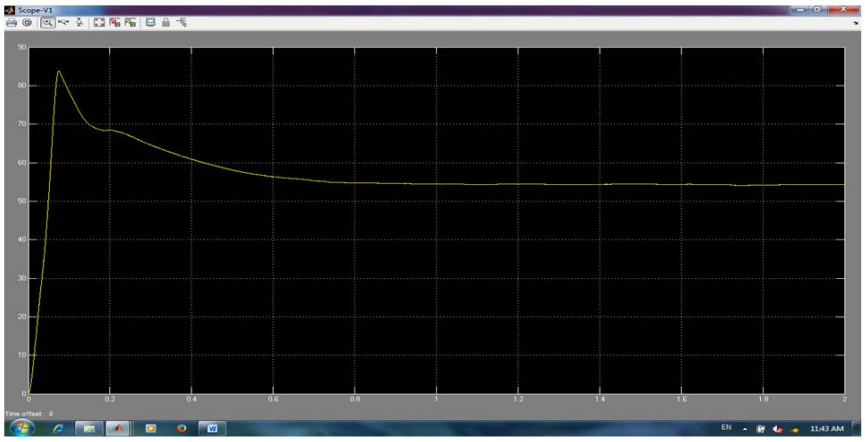

Fig. 3: Load side voltage to time

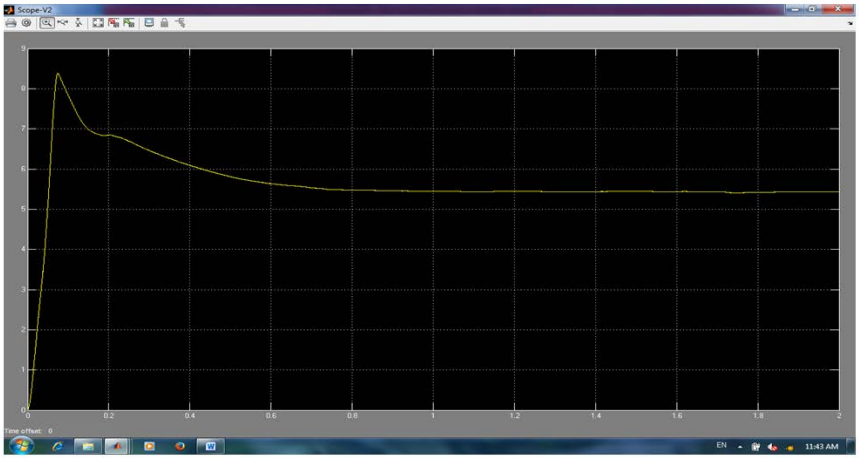

Fig. 4: Load side current wave form to time

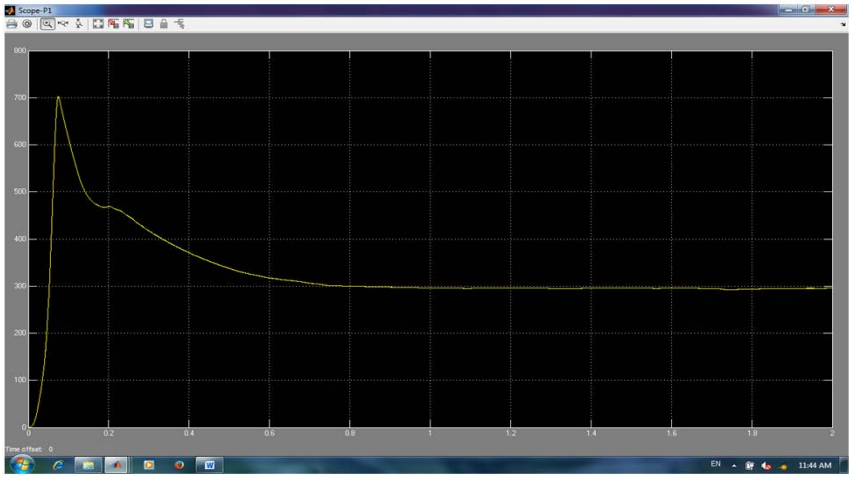

Fig. 5: Load side active power wave form to time

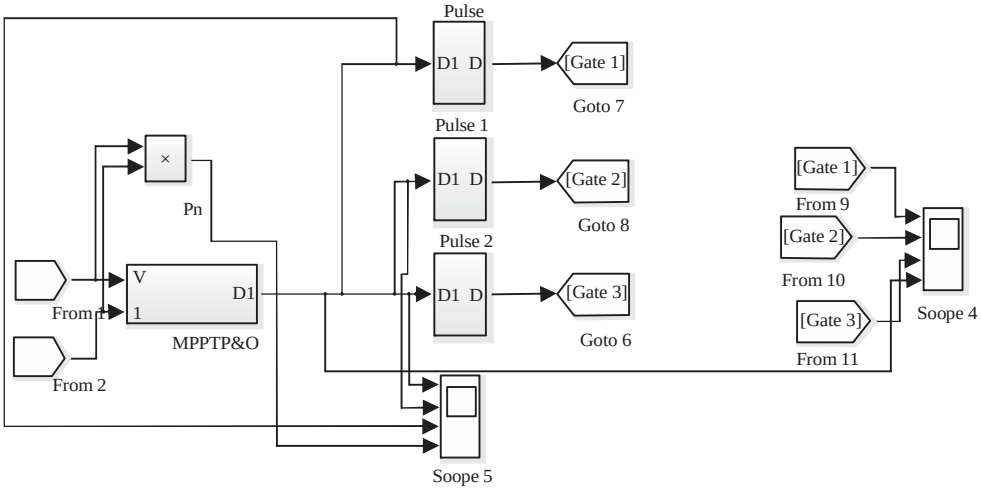

Fig. 6: Control circuit and MPPT circuit

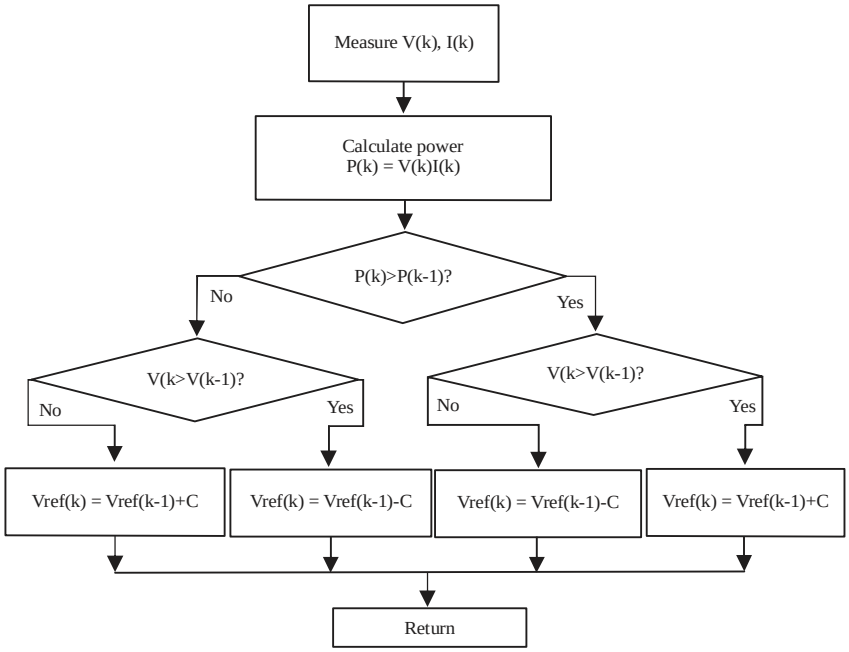

Fig. 7: Block of diagram MPPT

operator and gaining power to create pulses for MOSFTS control as observed, active fire control (0.8) and inactive fire control(0.2) exist (Fig. 6).

MPPT circuit and Maximum power point tracking: Output voltage and current have entered into MPPT from fuel cell and passed at the first from a voltage sampler and current sampler; sampling is made from signal due to this reason that it is the input signal of analog. To convert this signal to a digital signal, this block is used in other words at each step, the sample is taken from 0.0001sec of input signal and the signal is stored, not related to what change occurs in signal between these steps (Fig. 7 and 8).

After sampling, a previous step is stored and then the current and previous power is obtained by multiplying current by current and previous voltage and then difference of power and voltage between current and previous step is obtained. These are multiplied in a mathematical operator. Now two-position switch is placed; if multiplied difference of the current and previous power by current and previous voltage equals to a positive sign, the switch displays -1 at output if multiplied difference of current and previous power by current and previous voltage displays -1, the switch displays +1 at output. Then, it is multiplied by 0.001 which specifies the

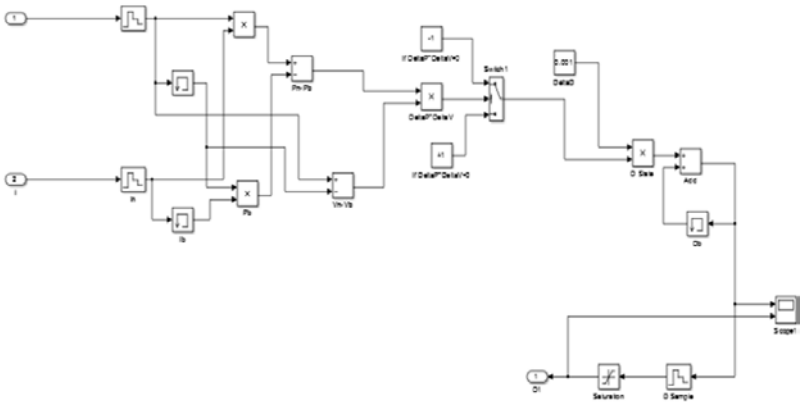

Fig. 8: Simulated MPPT circuit

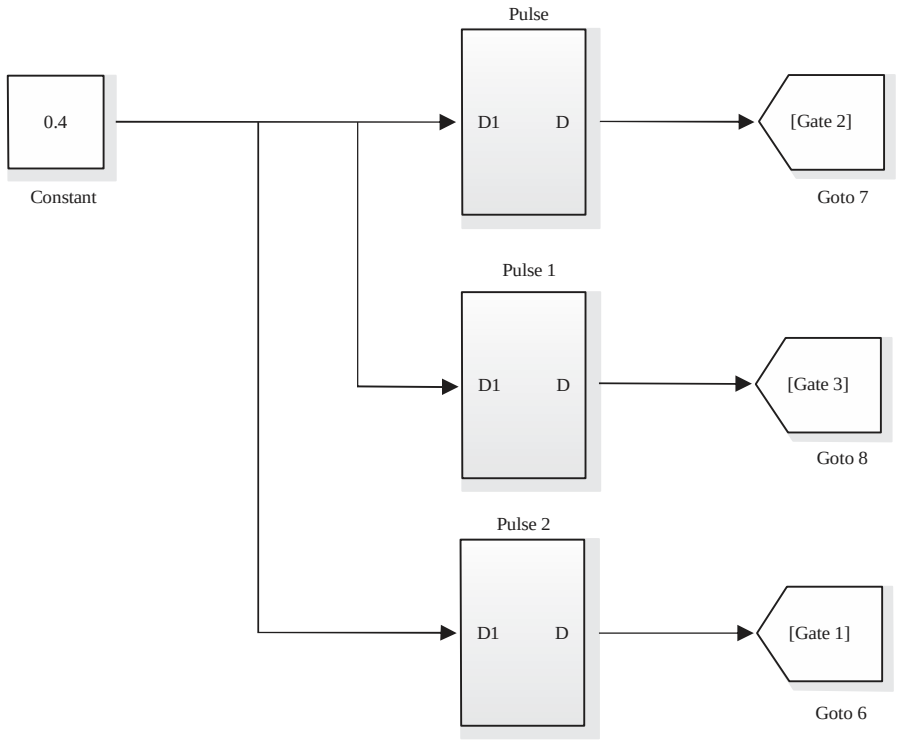

Fig. 9: Simulated circuit without MPPT

amount of changes, because the task cycle amount at each step changes by 0.001 in this simulation and then the obtained change amount which is +0.001 or -0.001 is summed with previous amount of task cycle or the previous step, so as to obtain the new task cycle amount. It passes from the sampler again in order that the digital signal converts to analog signal and at the end the limiter is used and this avoids going the task cycle amount beyond a certain limit because task cycle can just very between 0-1. If MPPT algorithm is not used and task cycle amount remains fixed on a certain amount (0.4), the power delivered by load equals (Fig. 9-11): As a result, the power delivered by load has increased using MPPT.

Output voltage, current and power of RL load: As observed in Fig. 12-14, it is observed that the cell is the result from favorable output power, current and voltage in resistive load. As observed in Fig. 12, output voltage has become 55 v. As observed in Fig. 13, output current

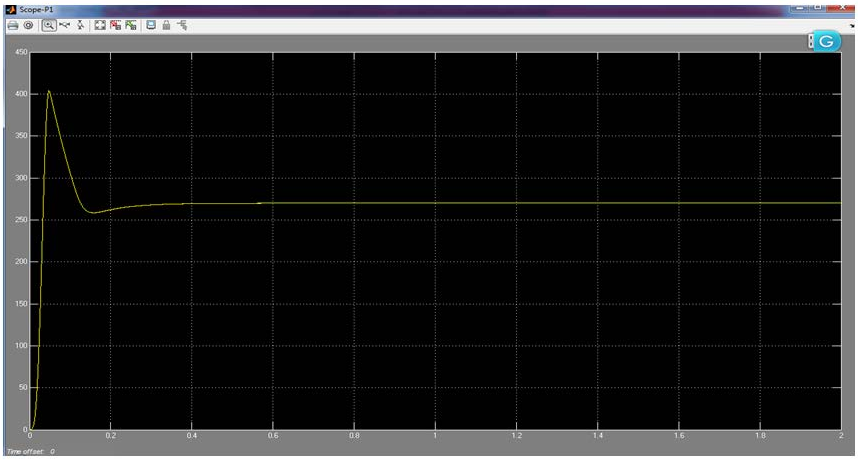

Fig. 10: Output power wave form to time without MPPT

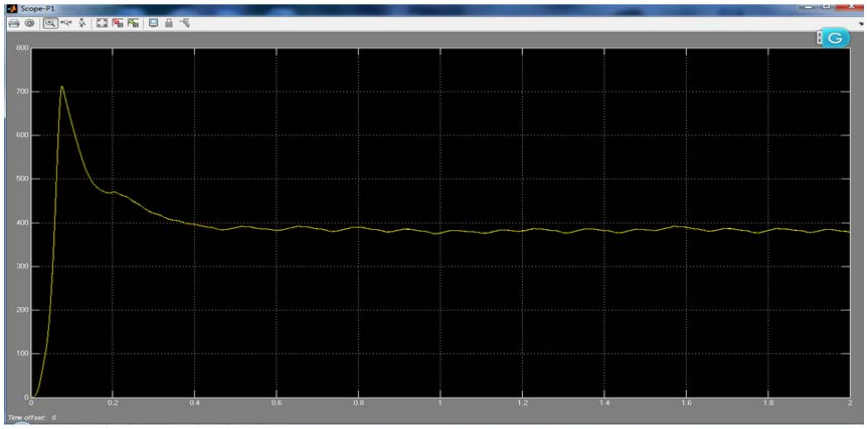

Fig. 11: Output power wave form to time with MPPT

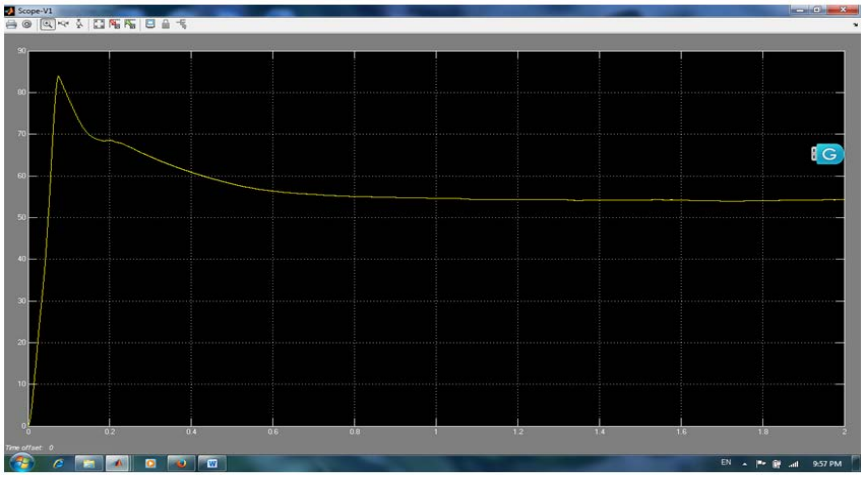

Fig. 12: Output voltage to time at RL load side

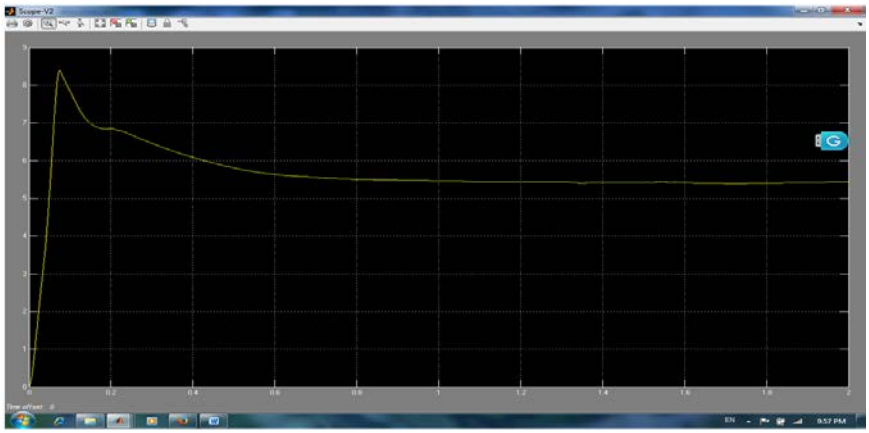

Fig. 13: Output current to time at RL load side

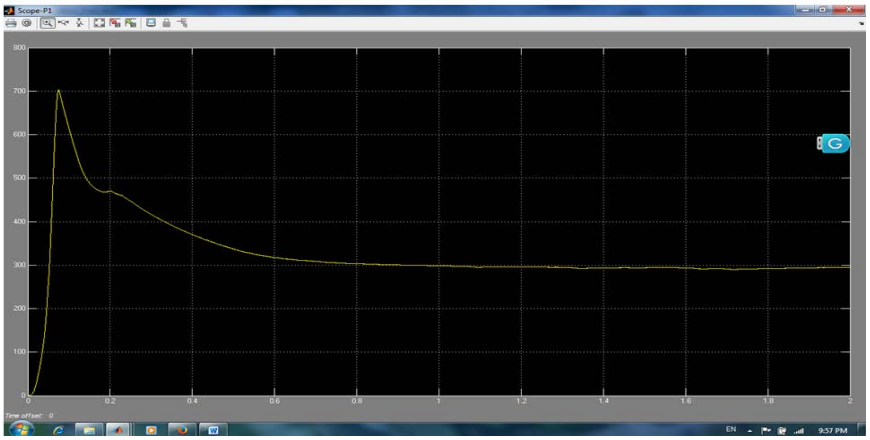

Fig. 14: Output power to time of RL load side

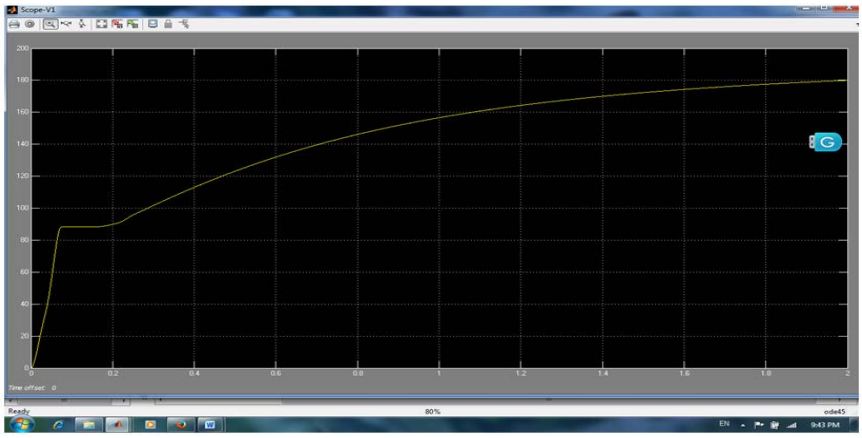

Fig. 15: output voltage to time of RLC load side

chart at RL load has equaled to 5.5 Amp which it is favorable. Further, output power has equaled to 300 W in Fig. 14.

Output power, current and voltage of RLC load: As observed in Fig. 15-17, the obtained output power, current and voltage is not favorable at resistance, inductance and

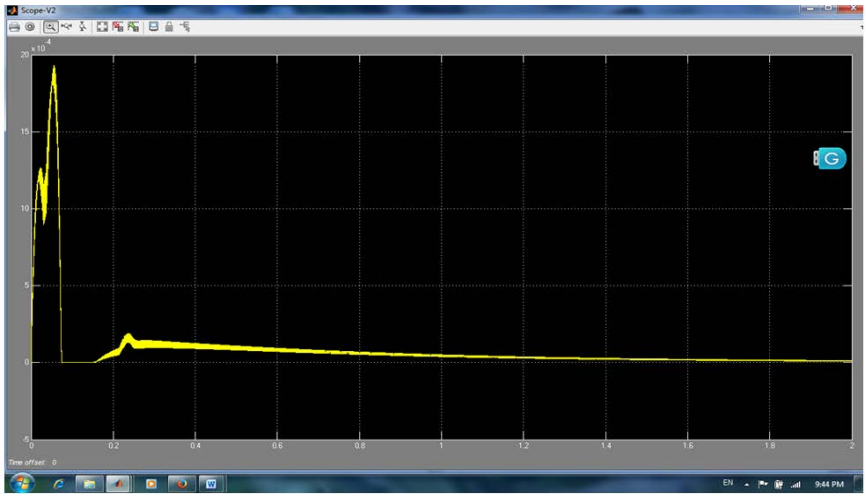

Fig. 16: Output current to time of RLC load side

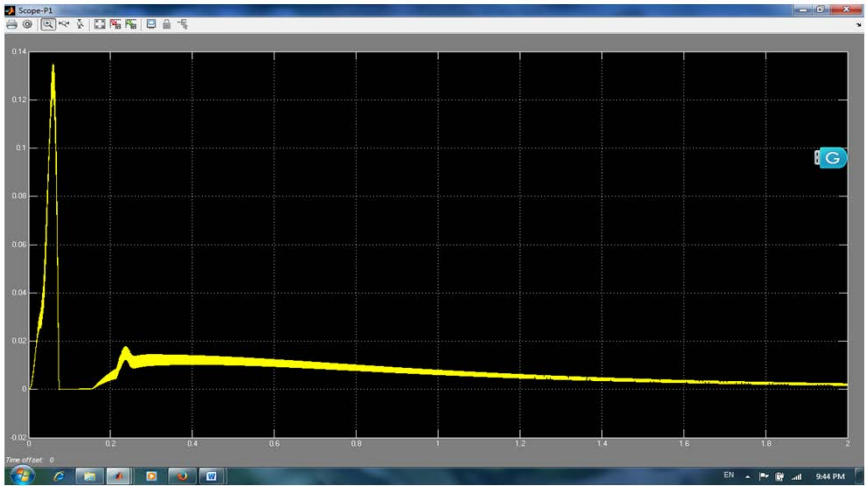

Fig. 17: Output power to time of RLC load side

capacitance load; the output power and current with severe fluctuations tend to 0. In Fig. 16, output current in RLC load tends to 0 which is not favorable. Further in Fig. 17, output power tends to 0 which is not favorable. Further in Fig. 17 output power trends to 0.

As a result as observed in figure, output of circuit is not favorable at RLC and RC but the result is more favorable at RL; comparison of RL with R indicates that if the resistive load remains pure, output power, voltage and current will be more favorable.

CONCLUSION

One of the most important characteristics of hybrid vehicles is reducing fuel consumption and emissions. In this regard with regard to adding additional equipment to conventional cars and considering the issues such as costs of design, construction and production, the cost of this type of vehicle goes up. One of policies to reduce the price of hybrid vehicles is to lower producers' profit. In industrialized countries such as America and Japan, the government has taken a series of facilities for producers and buyers and asked them to considered low profit. Further, on the other hand from perspective of saving fuel consumption, according to data obtained in industrialized countries with hybridizing internal combustion vehicles, annually 625 L of petrol is saved for each vehicle which is equivalent to 20% of price of car with typical internal combustion before hybridizing. Hybrid cars due to having economic justification, significant benefits and good efficiency and also reducing fossil reserves of the world will keep growing in future years. In this study,

interleaved two-phase boost converter has been considered. As known, the input current and Ripple of Boost DC-DC converter can reach to minimum by placement performance properties. In addition, the converter input current can be divided between various phases which this is suitable for heat waste. Thus, converter reliability can improve to a large extent. At the end, a MPPT method with layered converter boost model has been used to design fuel cell of electric vehicles. In this method, the microcontrollers have been used to design the circuit. MPPT technique has gained of the proton exchange between fuel cells layers and the simulated circuit with and without MPPT has been compared; further the simulation results for various loads have been examined. all the results and output waves form indicate solving the problem in ripple of high current via layered converters boost method.

REFERENCES

Benyahia, N., H. Denoun, A. Badji, M. Zaouia, T. Rekioua, N. Benamrouche and D. Rekioua, 2014. MPPT controller for an interleaved boost DC-DC converter used in fuel cell electric vehicles. Int. J. Hydrogen Energy, 39: 15196-15205.

Benyahia, N., H. Denoun, M. Zaouia, S. Tamalouzt and M. Bouheraoua *et al*., 2013. Characterization and control of supercapacitors bank for stand-alone photovoltaic energy. Energy Procedia, 42: 539-548.

Benyahia, N., T. Rekioua, N. Benamrouche, A. Bousbaine 2013. Fuel Cell Emulator for Supercapacitor Energy Storage Applications Electric Power Components and Systems 41: 569-585.

Dwari, S.M. and L. Parsa, 2007. A novel high efficiency high power interleaved coupled-inductor boost DC-DC converter for hybrid and fuel cell electric vehicle. Proceedings of the 2007 IEEE Vehicle Power and Propulsion Conference, September 9-12, 2007, IEEE, Arlington, Texas, pp: 399-404.

Ellabban, O., J. Van Mierlo and P. Lataire, 2011. A DSP-based dual loop digital controller design and implementation of a high power boost converter for hybrid electric vehicles applications. J. Power Electron., 11: 113-119.

Kim, J.S., G.Y. Choe, H.S. Kang and B.K. Lee, 2011. Robust low frequency current ripple elimination algorithm for grid-connected fuel cell systems with power balancing technique. Renewable Energy, 36: 1392-1400.

Rekioua, D. and E. Matagne, 2012. Optimization of Photovoltaic Power Systems: Modelization, Simulation and Control. Springer, London, England, ISBN:978-1-4471-2348-4, Pages: 283.

Rekioua, D., S. Bensmail and N. Bettar, 2014. Development of hybrid photovoltaic-fuel cell system for stand-alone application. Int. J. Hydrogen Energy, 39: 1604-1611.

Samosir, A.S. and A.H.M. Yatim, 2008. Implementation of new control method based on dynamic evolution control with linear evolution path for boost DC-DC converter. Proceedings of the 2008 IEEE 2nd International Power and Energy Conference, December 1-3, 2008, IEEE, Johor Bahru, Malaysia, pp: 213-218.

Samosir, A.S. and A.H.M. Yatim, 2010. Implementation of dynamic evolution control of bidirectional DC-DC converter for interfacing ultracapacitor energy storage to fuel-cell system. IEEE. Trans. Ind. Electron., 57: 3468-3473.

Samosir, A.S. and A.H.M. Yatim, 2011. Simulation and implementation of interleaved boost DC-DC converter for fuel cell application. Int. J. Power Electron. Drive Syst., 1: 168-174.

Seyezhai, R. and B.L. Mathur, 2012. Design and implementation of interleaved boost converter for fuel cell systems. Int. J. Hydrogen Energy, 37: 3897-3903.

Tang, Y., W. Yuan, M. Pan and Z. Wan, 2011. Experimental investigation on the dynamic performance of a hybrid PEM fuel cell/battery system for lightweight electric vehicle application. Applied Energy, 88: 68-76.

Thounthong, P., B. Davat, S. Rael and P. Sethakul, 2009. Fuel cell high-power applications. IEEE. Ind. Electron. Mag., 3: 32-46.

Torreglosa, J.P., F. Jurado, P. Garcia and L.M. Fernandez, 2011. Application of cascade and fuzzy logic based control in a model of a fuel-cell hybrid tramway. Eng. Appl. Artif. Intell., 24: 1-11.

Van Der Broeck, H. and I. Tezcan, 2006. 1 KW dual interleaved boost converter for low voltage applications. Proceedings of the 2006 CES/IEEE 5th International Power Electronics and Motion Control Conference, Vol. 3, August 14-16, 2006, IEEE, Shanghai, China, pp: 1-5.